

# RSC Advances



This is an *Accepted Manuscript*, which has been through the Royal Society of Chemistry peer review process and has been accepted for publication.

*Accepted Manuscripts* are published online shortly after acceptance, before technical editing, formatting and proof reading. Using this free service, authors can make their results available to the community, in citable form, before we publish the edited article. This *Accepted Manuscript* will be replaced by the edited, formatted and paginated article as soon as this is available.

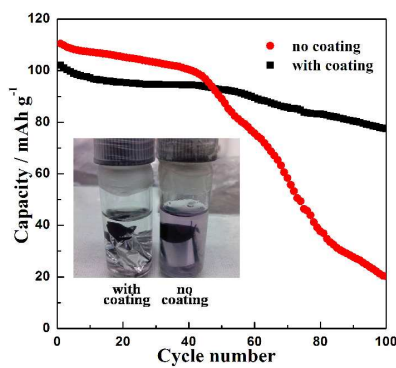
You can find more information about *Accepted Manuscripts* in the [Information for Authors](#).

Please note that technical editing may introduce minor changes to the text and/or graphics, which may alter content. The journal's standard [Terms & Conditions](#) and the [Ethical guidelines](#) still apply. In no event shall the Royal Society of Chemistry be held responsible for any errors or omissions in this *Accepted Manuscript* or any consequences arising from the use of any information it contains.

## Improved high temperature capacity retention of $\text{LiMn}_2\text{O}_4$ cathode lithium-ion battery by ion exchange polymer coating

Peng Xue,<sup>a</sup> Lei Pan,<sup>b</sup> Dacheng Gao,<sup>b</sup> Shengyang Chen,<sup>b</sup> Baofeng Wang<sup>a</sup>, Lei Li<sup>b\*</sup>

Ion exchange polymer coating on the  $\text{LiMn}_2\text{O}_4$  cathode to overcome capacity fading of lithium-ion battery at high temperature is first demonstrated, and it shows very good capacity retention compared with the pristine  $\text{LiMn}_2\text{O}_4$  cathode without coating.



Cite this: DOI: 10.1039/c0xx00000x

www.rsc.org/xxxxxxx

ARTICLE TYPE

## Improved high temperature capacity retention of LiMn<sub>2</sub>O<sub>4</sub> cathode lithium-ion battery by ion exchange polymer coating

Peng Xue,<sup>a</sup> Dacheng Gao,<sup>b</sup> Shengyang Chen,<sup>b</sup> Shuyu Zhao,<sup>b</sup> Baofeng Wang<sup>a</sup> and Lei Li<sup>b\*</sup>

Received (in XXX, XXX) XthXXXXXXXXXX 20XX, Accepted Xth XXXXXXXXXXXX 20XX

DOI: 10.1039/b000000x

**Ion exchange polymer coating on the LiMn<sub>2</sub>O<sub>4</sub> cathode to overcome capacity fading of lithium-ion battery at high temperature is first demonstrated, and it shows very good capacity retention compared with the pristine LiMn<sub>2</sub>O<sub>4</sub> cathode without coating.**

Rechargeable lithium-ion batteries (LIBs) are expected to be used as the power source for hybrid electric vehicles (HEVs), plug-in hybrid electric vehicles (EVs) and electric vehicles due to their high intrinsic energy density and high voltage.<sup>1</sup> However, the current LIBs technologies are not yet able to meet the requirement of efficiently storing alternative energy sources and / or powering hybrid or electric vehicles. Enhancement in safety and long life, reduction in cost, and improvement in thermal stability and energy density are the main properties that have to be implemented. To meet the above requirements, many research groups have extensively and intensively investigated many possible cathode materials such as LiCoO<sub>2</sub>,<sup>2</sup> LiNi<sub>1-x-y</sub>Co<sub>x</sub>Mn<sub>y</sub>O<sub>2</sub>,<sup>3</sup> LiFePO<sub>4</sub><sup>4</sup> and LiMn<sub>2</sub>O<sub>4</sub><sup>5-7</sup> for the applications in EVs. Among the well-studied cathode materials, the LiMn<sub>2</sub>O<sub>4</sub> (LMO) with the spinel framework has been considered as one of the most promising cathode materials to be used for EVs due to several advantages desirable for large-scale LIBs applications: (1) low costs and abundance of its raw materials, (2) high rate performance due to its three dimensional (3D) channel structure that facilitates efficient Li<sup>+</sup> diffusion, (3) high safety and non-toxicity, and (4) a high operation potential (~4.1 V vs. Li/Li<sup>+</sup>).<sup>1</sup> However, serious capacity fading of the LIBs based on the LMO especially at high temperature over 55 °C is still a big barrier to practical applications.<sup>5-7</sup> The capacity fading is known to be caused by the dissolution of Mn<sup>2+</sup> from the LMO into the electrolyte, which is originated from the disproportionation reaction: 2Mn<sup>3+</sup> (s) → Mn<sup>4+</sup> (s) + Mn<sup>2+</sup> (aq).<sup>5,6</sup> Also, it has been known that dissolution accelerated in the high voltage range of > 4.0 V vs. Li/Li<sup>+</sup> and also by the attack of hydrogen fluoride (HF), inevitably formed by both thermal decomposition of lithium hexafluorophosphate (LiPF<sub>6</sub>) and the reaction of the LiPF<sub>6</sub> with residual water in the electrolyte.<sup>5-7</sup> Mn<sup>2+</sup> is soluble in the non-aqueous electrolyte and Mn<sup>4+</sup> tends to stay in the positive electrode in a form of λ-MnO<sub>2</sub>. While the solvated Mn<sup>2+</sup> is readily reduced at the negative electrode because the redox potential of Mn<sup>2+</sup>/Mn couple is much higher than the intercalation potential of the carbonaceous negative electrode materials. Then, the deposition of Mn metal on the carbon surface will lead to the

significant impedance rise and capacity fading of the LIBs.

In order to suppress Mn<sup>2+</sup> dissolution, a lot of methods are reported: (1) partial Mn substitution with different transition metals such as Li<sup>+</sup>, Mg<sup>2+</sup> and Al<sup>3+</sup>,<sup>8</sup> (2) partial anion substitution O<sup>2-</sup> with F,<sup>9</sup> (3) metal oxide surface coatings,<sup>10</sup> (4) functional electrolyte additives,<sup>11</sup> (5) new polymer binders,<sup>12</sup> and (6) new non-fluorinated lithium salts such as lithium bisoxalato borate (LiBOB).<sup>13</sup> Despite an improved cycling performance, many of these approaches also lead to additional drawbacks, such as the sacrifice of the specific capacity, or involve more complex steps which will increase the production cost.

Herein, we report a simple method to solve the Mn<sup>2+</sup> dissolution problem by coating cation exchange polymer on the surface of LMO cathode electrode. Through ion exchange reaction, H<sup>+</sup> ions of the cation exchange polymer will be replaced by the dissolved Mn<sup>2+</sup> ions of LMO electrodes (shown in Fig. 1). Then the dissolved Mn<sup>2+</sup> ions will be captured by the cation exchange polymer, resulting in improved cycle performance at high temperature. In addition, the cation exchange polymers are normally considered as a single conductor (or ion conducting electrolyte) used in lithium-ion battery<sup>14</sup> and lithium-sulfur battery.<sup>15</sup> Thus, Li<sup>+</sup> ions diffusion in the cell is not affected.

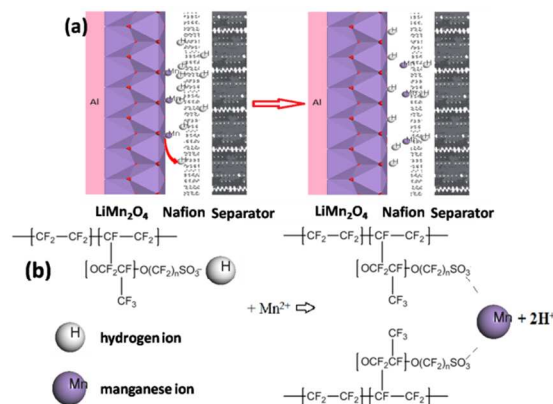


**Fig. 1** (a) Schematic diagram for the principle of cation exchange polymer coating on LiMn<sub>2</sub>O<sub>4</sub> electrode to capture dissolved Mn<sup>2+</sup> ions. (b) Ion exchange reaction between H<sup>+</sup> ions on Nafion ionomer and Mn<sup>2+</sup> ions.

In our experiments, Nafion ionomer made by Dupont, one of the best known cation exchange polymer is used as the ion exchange polymer coating on the LMO electrodes. The LMO electrode was composed with LiMn<sub>2</sub>O<sub>4</sub> powder (80 wt%), carbon

black (10 wt%) and poly(vinylidene fluoride) (PVDF 10 wt%). The detailed experimental process is described in the ESI. Nafion dispersion (Nafion dispersion D520, 5 wt% in alcohol/water) solution was coated on the LMO electrode, and dried at room temperature to make a Nafion coated electrode. The amount of Nafion on the electrode is about  $0.56 \text{ mg cm}^{-2}$ .

In order to verify the ion exchange reaction between the dissolved  $\text{Mn}^{2+}$  ions in electrolyte and  $\text{H}^+$  ions of cation exchange polymer, two experiments were carried out. First, both the LMO electrodes with and without Nafion coating were put in a sealed bottle containing a 1.0 M  $\text{LiPF}_6$ -dissolved EC-DMC (1:1, v:v) electrolyte at  $55^\circ\text{C}$  for 15 days. From Fig. 2a, it can be easily found that the solution soaked in the LMO electrode with Nafion coating is a transparent and colorless solution, however, the solution soaked in the LMO electrode without coating shows a pink color, which is normally the color of bivalent manganese ions. The manganese concentration of the electrolyte solution in the electrode with Nafion coating ( $0.123 \text{ mg L}^{-1}$ ) is very smaller than that of the electrode without Nafion coating ( $1.684 \text{ mg L}^{-1}$ ). These results indicate that the Nafion coating blocked the  $\text{Mn}^{2+}$  ions into the electrolyte, thereby inhibiting the disproportionation reaction of the  $\text{Mn}^{3+}$  ions. In addition, it also implies that the Nafion coating will be as an effective layer to prevent the LMO electrode by the attack of HF formed by decomposition of  $\text{LiPF}_6$  salt in electrolyte. The occurrence of ion exchange reaction was further supported by the FT-IR spectra of Nafion film obtained before and after storage in the manganese-dissolved electrolyte. In the Nafion with  $\text{H}^+$  form, the band at  $972 \text{ cm}^{-1}$  was assigned to  $-\text{SO}_3\text{H}$  group.<sup>16</sup> However, the intensity of this band decreased when the part of  $\text{H}^+$  ions were exchanged by  $\text{Mn}^{2+}$  ions. The band at  $1057 \text{ cm}^{-1}$  of the Nafion with  $\text{H}^+$  form was attributed to the  $-\text{SO}_3^-$  symmetric stretch.<sup>16,17</sup> Due to the interaction between  $\text{Mn}^{2+}$  and oxygen, this band shifted to  $1060 \text{ cm}^{-1}$  of the Nafion captured  $\text{Mn}^{2+}$  ions.

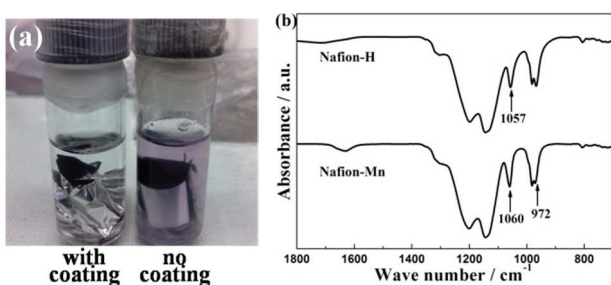


Fig. 2 (a) Image of solutions of  $\text{LiMn}_2\text{O}_4$  electrodes with and without Nafion coating soaked in electrolytes at  $55^\circ\text{C}$  for 15 days. (b) FT-IR spectra of Nafion film obtained before (Nafion-H) and after (Nafion-Mn) storage in the manganese-dissolved electrolyte.

The typical morphologies of the LMO electrodes with and without Nafion coating are shown in Fig. 3. Compared with the pristine electrode shown in Fig. 3a, it can be clearly seen that a visible Nafion layer is homogeneously formed on the LMO electrode after coated Nafion solution. The thickness of the Nafion layer was about  $1 \mu\text{m}$ . The Nafion layer could not only have the advantage of blocked the  $\text{Mn}^{2+}$  ions into the electrolyte, but also prevent the active material by the attack of HF formed by the decomposition of  $\text{LiPF}_6$ . To analyze the morphology changes of the electrode after charge/discharge cycling measurements, the

cells were disassembled in an argon-filled glove box. The electrodes were washed with anhydrous DMC several times to remove residual salts, and then dried in vacuum over for 2 h at room temperature. It can be seen from Fig. 3c that except for a little cracks, most of Nafion coating remains integrity after cycling measurements, implying the stability of the Nafion layer during charge/discharge cycling measurements. Fig. 3d shows the TG curve of the LMO electrodes with Nafion coating before and after cycling measurements. In both electrodes, the weight loss between  $300$  and  $550^\circ\text{C}$  is about  $16.5 \text{ wt}\%$ , which is mainly due to the degradation of PVDF binder and Nafion coating in both electrodes. TG curves of both electrodes before and after 100 cycling test show almost same, which indicates that Nafion layer has good stability on the electrodes during charge/discharge cycling measurements.

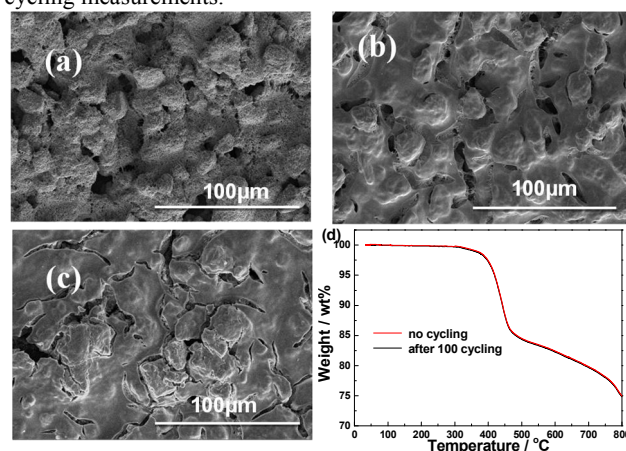
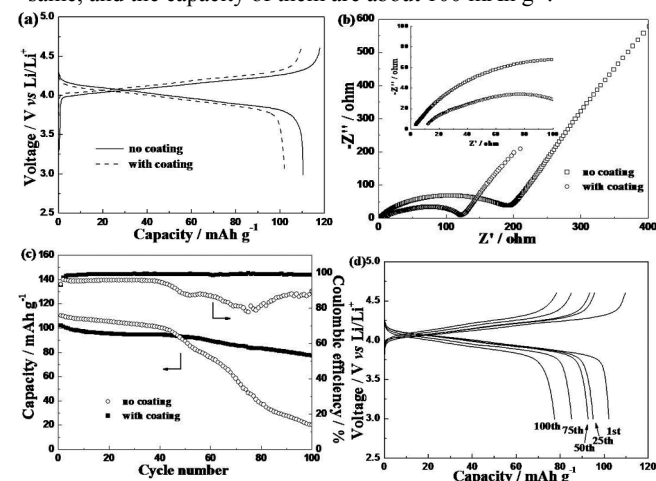


Fig. 3 SEM images of  $\text{LiMn}_2\text{O}_4$  electrodes without Nafion coating (a), with Nafion coating (b) and after 100 cycles (c). TG curves of  $\text{LiMn}_2\text{O}_4$  electrodes with Nafion coating before and after 100 cycles (d).

Initial charge-discharge profiles of the cells using both the LMO electrodes at  $55^\circ\text{C}$ , which were cycled under a voltage range of  $3.0\text{--}4.5 \text{ V}$  at current density of  $100 \text{ mA g}^{-1}$ , were shown in Fig. 4a. Two pseudoplateaus at around  $3.9$  and  $4.1 \text{ V}$  that indicate the typical electrochemical behaviour of the spinel  $\text{LiMn}_2\text{O}_4$  were observed in both charge and discharge curves.<sup>18</sup> The performance of the first cycle of the cell using the pristine LMO electrode (charge capacity:  $118.0 \text{ mAh g}^{-1}$ , discharge capacity:  $110.5 \text{ mAh g}^{-1}$ , coulombic efficiency:  $93.6\%$ ) was better than that of the cell using the LMO electrode with Nafion coating (charge capacity:  $109.6 \text{ mAh g}^{-1}$ , discharge capacity:  $102.1 \text{ mAh g}^{-1}$ , coulombic efficiency:  $93.2\%$ ). The main reason is the ohmic resistance based on AC impedance measurements shown in Fig. 4b, increases from  $3.74 \Omega \text{ cm}^2$  to  $12.27 \Omega \text{ cm}^2$  with the Nafion coating on the electrodes due to the low conductivity of Nafion film (about  $10^{-5} \text{ S cm}^{-1}$ ). The detailed analysis of AC impedance results is described in the ESI.

The cycling performance of the cells using both the LMO electrodes at  $55^\circ\text{C}$  is shown in Fig. 4c. It can be found that the capacities of both cells decrease with the increment of cycle numbers. For the pristine LMO electrode, the capacity reduced rapidly after around 40 cycles, and was decreased to  $20.2 \text{ mAh g}^{-1}$  ( $18.3\%$  of the initial capacity) after 100 cycles. Compared to the pristine LMO electrode, the battery using the LMO electrode with Nafion coating showed a high capacity retention of  $77.4 \text{ mAh g}^{-1}$

(75.8% of the initial capacity) after 100 cycles. The coulombic efficiency of the LMO electrode with Nafion coating was almost 100% even after 100 cycles, which is also better than that of the battery using the pristine LMO electrode. In addition, the difference between the charge potential and discharge potential of the LMO electrode with Nafion coating shown in Fig. 4d does not change too much compared with the pristine LMO electrode (see Fig. S3). In general, there are two main factors leading to the capacity fading of LMO electrodes at high temperature, including the disproportionation reaction of LMO and LiPF<sub>6</sub> based electrolyte.<sup>6</sup> At room temperature, both the disproportionation reaction and thermal decomposition of LiPF<sub>6</sub> salt will not be easily occurred. Then both cells using both the LMO electrodes show good cycling performance at room temperature (Fig. S4). After 100 cycles, the capacity retention of both cells are almost same, and the capacity of them are about 100 mAh g<sup>-1</sup>.



**Fig.4** Electrochemical performance of batteries at 55 °C. (a) Voltage profiles for the first cycle of the batteries using LiMn<sub>2</sub>O<sub>4</sub> electrodes with and without Nafion coating measured between 3.0 and 4.5 V at a current density of 100 mA g<sup>-1</sup>. (b) Nyquist plots of LiMn<sub>2</sub>O<sub>4</sub> electrodes with and without Nafion coating after the first 100 mA g<sup>-1</sup> charged cell. (c) Cycling stability of batteries using LiMn<sub>2</sub>O<sub>4</sub> electrodes with and without Nafion coating. Current density: 100 mA g<sup>-1</sup>. (d) Charge-discharge curves of battery using LiMn<sub>2</sub>O<sub>4</sub> electrodes with Nafion coating at different cycle numbers.

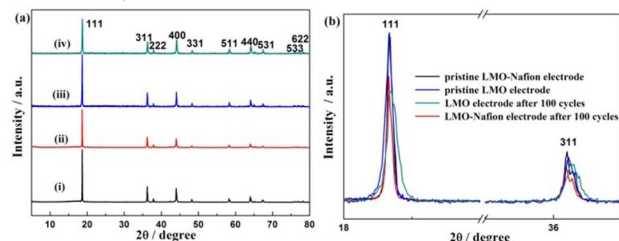


**Fig.5** XRD patterns of LiMn<sub>2</sub>O<sub>4</sub> electrodes (a) and the magnified between 18 to 37 for 2θ (b): pristine LiMn<sub>2</sub>O<sub>4</sub> electrodes with Nafion coating (i), and after 100 cycles (ii), pristine LiMn<sub>2</sub>O<sub>4</sub> electrodes without Nafion coating (iii) and after 100 cycles (iv).

Fig. 5 shows the XRD patterns of the pristine and LMO electrodes after 100 cycles with and without Nafion coating at 55 °C. All the peaks in the XRD patterns of the LMO electrodes were indexed as the spinel phase (JCPDS file No. 35-0782). It

can be found that the intensities of all the LiMn<sub>2</sub>O<sub>4</sub> diffraction peaks of both LMO electrodes are weakened. This is maybe due to the decay of the spinel structure of LiMn<sub>2</sub>O<sub>4</sub> which resulted from Mn<sup>2+</sup> dissolution at elevated temperature.<sup>7</sup> However, the extent of weakening of the electrode without coating is stronger than that of the electrode with coating. Fig. 5b shows the magnified patterns at 2θ = 18-37°. It can be found that both the diffraction peaks (111) and (311) of the electrode without coating shifted to higher angle after cycled. In addition, the value of full width at half maxima (FWHM) of both peaks also increased after cycled. These results suggest that the crystal lattice of the LiMn<sub>2</sub>O<sub>4</sub> in the electrode without coating shrank after cycled.<sup>6,7</sup> Compared with the LMO electrode without coating, there no obvious change of the FWHM value and no obvious shift were found in the diffraction peaks of the electrode with Nafion coating even after 100 cycles, which indicates that the extent of degradation of the spinel structure of LiMn<sub>2</sub>O<sub>4</sub> in the electrode without coating is much stronger than that of the electrode with coating. These results indicate that the Nafion coated LMO electrode shows very better thermal stability than that of the pristine LMO electrode.

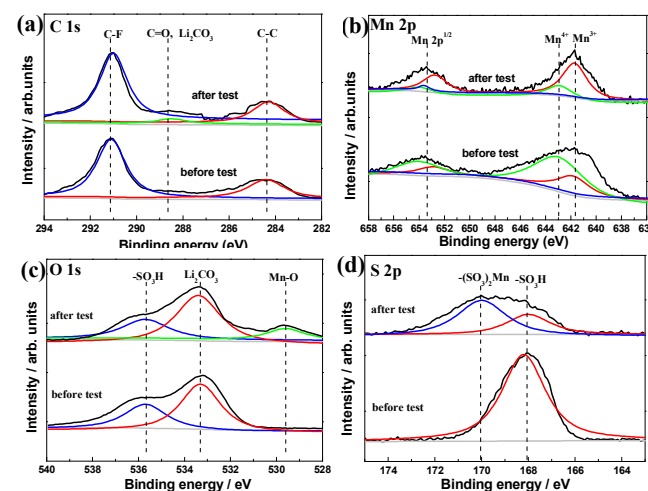


**Fig.6** XPS spectra of LiMn<sub>2</sub>O<sub>4</sub> electrodes with Nafion coating before and after 100 cycles at 55 °C. (a) C 1s spectra, (b) Mn 2p spectra, (c) O 1s spectra and (d) S 2p spectra.

The surfaces of the LiMn<sub>2</sub>O<sub>4</sub> electrodes with Nafion coating before and after 100 cycles at 55 °C were analyzed by XPS. The C 1s, Mn 2p, O 1s and S 2p spectra of both electrodes are shown in Fig. 6. The C 1s spectra show slight difference between the LiMn<sub>2</sub>O<sub>4</sub> electrodes with Nafion before and after test (see Fig. 6a). There are two characteristic peaks in both electrodes in the C 1s spectra: C-C bond in carbon black (284.1 eV)<sup>19</sup>, C-F bond in Nafion and PVDF (284.2eV)<sup>20</sup>. In addition, new peak attributing to Li<sub>2</sub>CO<sub>3</sub> (288.7 eV) can be found in the LiMn<sub>2</sub>O<sub>4</sub> electrodes after test, which is due to SEI formation on the electrodes during the cycling measurements.<sup>19,21</sup>

The Mn 2p spectra are shown in Fig. 6b. There are two main peaks in Mn 2p spectra in both electrodes, dominated by Mn 2p<sup>3/2</sup>: Mn<sup>3+</sup> in Mn<sub>2</sub>O<sub>3</sub> or LiMn<sub>2</sub>O<sub>4</sub> (641.7 eV), Mn<sup>4+</sup> in MnO<sub>2</sub> or LiMn<sub>2</sub>O<sub>4</sub> (642.9 eV).<sup>22</sup> And a weak new Mn 2p<sup>1/2</sup> peak (653.6 eV) is appeared in the tested LiMn<sub>2</sub>O<sub>4</sub> electrode.<sup>22</sup> This shows that the Nafion film can capture of Mn<sup>2+</sup> ions on the electrodes.

In the O 1s spectra in both electrodes shown in Fig. 6c, there are two main peaks:  $-\text{SO}_3\text{H}$  bond in Nafion (535.7 eV)<sup>20</sup> and  $\text{Li}_2\text{CO}_3$  (532.0 eV)<sup>23</sup>. In addition, Mn-O bond in  $-(\text{SO}_3)_2\text{Mn}$  (529.6 eV)<sup>21</sup> can be found in the electrodes after test, which indicates that Nafion layer can capture the  $\text{Mn}^{2+}$  from the  $\text{LiMn}_2\text{O}_4$  electrode.

The S 2p spectra are shown in Fig. 6d. There is only one main peak in S 2p spectra in the electrodes before test, which is dominated by  $-\text{SO}_3\text{H}$  bond (168.1 eV).<sup>24</sup> For the electrode after test, a new peak attributing to  $-(\text{SO}_3)_2\text{Mn}$  (170.8 eV)<sup>24</sup> can be found, which is also indicates that Nafion layer can capture the  $\text{Mn}^{2+}$  from the  $\text{LiMn}_2\text{O}_4$  electrode.

In summary, a simple electrode modification method using ion exchange polymer coating is reported to overcome severe capacity fading of the  $\text{LiMn}_2\text{O}_4$  cathode lithium-ion batteries at high temperature. The Nafion coating layer will not only block the  $\text{Mn}^{2+}$  ions into the electrolyte, but also be as an effective layer to prevent the LMO electrode by the attack of HF formed by the decomposition of  $\text{LiPF}_6$  salt in electrolyte. Thus, the LMO electrodes after Nafion coating show very good high capacity retention at 55 °C compared with the pristine LMO electrodes. We expect this new method may be readily applicable for commercial LMO cathode LIB products. Further work on the choice and synthesis of ion exchange polymer, optimization of the loading of ion exchange polymer and coating process is under investigation.

This work was supported by the National Natural Science Foundation of China (20904031), Natural Science Foundation of Shanghai (14ZR1422100), and Shanghai key lab of polymer dielectrics (Shanghai key lab of electrical insulation and thermal aging). Thanks for Instrumental Analysis Center of Shanghai Jiaotong University.

## Notes and references

<sup>a</sup>Shanghai University of Electric Power, Shanghai 200090, China.

<sup>b</sup>School of Chemistry and Chemical Engineering, Shanghai Jiaotong University, Shanghai 200240, China. E-mail: lilei0323@sjtu.edu.cn

† Electronic Supplementary Information (ESI) available: Details of experimental procedures. See DOI: 10.1039/b000000x/

1 J.-M. Tarascon and M. Armand, *Nature*, 2001, **414**, 359.

2 E. Antolini, *Solid State Ionics*, 2004, **170**, 159.

3 N. Yabuuchi and T. Ohzuku, *J. Power Sources*, 2003, **119-121**, 171.

4 A. Deb, U. Bergmann, E. J. Cairns and S. P. Cramer, *J. Phys. Chem. B*, 2004, **108**, 7046.

5 A. Blyr, C. Sigala, G. Amatucci, D. Guyomard, Y. Chabre and J.M. Tarascon, *J. Electrochem. Soc.*, 1998, **145**, 194.

6 F.T. Quinlan, K. Sano, T. Willey, R. Vidu, K. Tasaki and P. Stroeve, *Chem. Mater.*, 2001, **13**, 4207.

7 J. Shim, R. Kostecki, T. Richardson, X. Song and K.A. Striebel, *J. Power Sources*, 2002, **112**, 222.

8 Y. K. Sun, C. S. Yoon, C. K. Kim, S. G. Youn, Y. S. Lee, M. Yoshio and I. H. Oh, *J. Mater. Chem.*, 2001, **11**, 2519.

9 Y. K. Sun, M. J. Lee, C. S. Yoon, J. Hassoun, K. Amine and B. Scrosati, *Adv. Mater.*, 2012, **24**, 1192.

10 Y. C. Sun, Z. X. Wang, L. Q. Chen and X. J. Huang, *J. Electrochem. Soc.*, 2003, **150**, 1294.

11 I. H. Cho, S. S. Kim, S. C. Shin and N. S. Choi, *Electrochem. Solid State Lett.*, 2010, **13**, 168.

12 M.-H. Ryou, S. Hong, M. Winter, H. Lee and J. W. Choi, *J. Mater. Chem. A*, 2013, **1**, 15224.

13 M. S. Whittingham, *Chem. Rev.*, 2004, **104**, 4271.

14 H. Liang, X. Qiu, S. Zhang, W. Zhu and L. Chen, *J. Appl. Electrochem.*, 2004, **34**, 1211.

15 Q. Tang, Z. Shan, L. Wang, X. Qin, K. Zhu, J. Tian and X. Liu, *J. Power Sources*, 2014, **246**, 253.

16 R. Buzzoni, S. Bordiga, G. Ricchiardi, G. Spoto and A. Zecchina, *J. Phys. Chem.*, 1995, **99**, 1937.

17 M. Falk, *Can. J. Chem.*, 1980, **58**, 1495.

18 H.-W. Lee, P. Muralidharan, R. Ruffo, C. M. Mari, Y. Cui and D. K. Kim, *Nano. Lett.*, 2010, **10**, 3852.

19 M. Q. Xu, L. S. Hao, Y. L. Liu, W. S. Li, L. D. Xing and B. Li, *J. Phys. Chem. C*, 2011, **115**, 6087.

20 C. Chen, G. Levitin, D. W. Hess and T. F. Fuller, *J. Power Sources*, 2007, **169**, 290.

21 Y. Kusachi, Z. C. Zhang, J. Dong and K. Amine, *J. Phys. Chem. C*, 2011, **115**, 24013.

22 N. Treuil, C. Labrugere, M. Menetrier, J. Portier, G. Gampet, A. Deshayes, J.C. Frison, S. J. Hwang, S. W. Song and J. H. Choy, *J. Phys. Chem. B*, 1999, **103**, 2100.

23 L. Zhou, S. Dalavi, M. Q. Xu and B. Lucht, *J. Power Sources*, 2011, **196**, 8073.

24 M. Schulze, M. Lorenz, N. Wagner and E. Gülzow, *Fresenius J. Anal. Chem.*, 1999, **365**, 106.